CORROSION BEHAVIOUR OF WELDED HR3C STEEL UNDER SUPERCRITICAL WATER CONDITIONS

Monika HRADILOVÁ [a], Eliška KŘEČANOVÁ [a], Zuzana SKOUMALOVÁ [b], Jan MACÁK [c], Václav BYSTRIANSKÝ [c], Markéta ZYCHOVÁ [a]

[a] *Centre for Research Rez s.r.o., Husinec-Rez, Czech Republic, EU, hri@cvrez.cz*
[b] *UJV Rez, Husinec-Rez, Czech Republic, EU*
[c] *Institute of Chemical Technology Prague, Department of Power Engineering, Prague, Czech Republic, EU*

Abstract

Supercritical water (SCW) is a promising medium with a broad spectrum of potential applications in the industry. However, the absence of appropriate structural material able to withstand the severe corrosive conditions of SCW still limits its utilization. Therefore, this work is focused on broadening of data related to corrosion behaviour of HR3C steel under supercritical water conditions. The HR3C is austenitic steel with a good high temperature corrosion resistance and creep strength in flue gas environment. The studied samples of HR3C with weld joint were exposed under conditions of SCW (600 °C and 25 MPa) up to 1000 h. Subsequently, the corrosion rate was evaluated on the basis of measured weight changes of the samples. The effect of SCW on the microstructure stability was verified via light, electron microscopy and measurement of microhardness. The oxide layers formed during the expositions were further analyzed by measurements of electrochemical impedance spectroscopy as well as by the X-ray photoelectron and Raman spectroscopy. The preliminary results reveal that studied material exhibit very good corrosion resistance under conditions of SCW.

Keywords: supercritical water, austenitic steel, weld, electrochemical impedance spectroscopy

1. INTRODUCTION

Water above its critical point (374 °C and 22 MPa) is called supercritical water (SCW) [1] and can be effectively used in wide spectrum of industrial application [1, 2]. SCW can be utilized in (i) oxidation reactions, (ii) conversion of organic compounds to gaseous or liquid products, (iii) organic and inorganic synthesis processes and (iv) in power plants as a more effective heat transfer working fluid. Besides, SCW becomes severe corrosive medium. Recently, the structural materials that would be used under SCW conditions are still under investigation [3].

Advanced commercial austenitic steels such as HR3C have been developed for application at power plant boilers operating at temperatures above 500 °C [4, 5, 6]. HR3C steel containing higher amount of chromium (~25 wt.%) and nickel (~20 wt.%) has been designated for application requiring mainly improved corrosion and oxidation resistant [7]. In addition, it exhibits better creep strength than martensitic steels [8]. Austenitic HR3C steel is characterized by good stability of microstructure, which is additionally achieved by nitrogen-rich Nb-based precipitates. These precipitates are responsible for other increase of steel strengthening. However, during long term exposition at temperatures above 600 °C the brittle σ phase may be formed within the structure and it may degrade the mechanical properties [9, 10].

However, this steel remains to be very promising material and therefore this work was performed in order to study the effect of SCW on the corrosion behaviour of austenitic stainless steel HR3C.

2. EXPERIMENTAL DETAILS

Corrosion behaviour of welded HR3C steel samples was studied under conditions of SCW. The chemical composition of austenitic HR3C steel was validated by optical emission spectrometry (ARCMET 8000 SL Mobile Lab). The results of this analysis are summarized in the **Table 1**.

Table 1 The chemical composition of HR3C

Wt. %	C	Si	Mn	P	S	Cr	N	Ni	Nb	Fe
HR3C	0.05	0.46	1	0.03	0.001	25.9	0.25	20	0.25	Bal.

The initial microstructure was studied by light microscope (LM; Nikon Epiphot 300). For this purpose, the samples were prepared by mechanical grinding with papers up to 2400, mechanical polishing with diamante paste 1, 3 μm and oxide polishing suspension. This was followed by electrolytical etching with 10 % oxalic acid. The dimensions of the samples were approximately 2, 18 and 50 mm. Before exposition, the samples were decreased by ethanol and acetone and weighed to estimate the corrosion rate. The microhardness measurements were performed by using a Anton Paar MHT 4 microhardness tester before and after the longest (1000 h) exposition. The microhardness profile was measured with loading of 100 g for 10 s.

The samples of studied steel were exposed to supercritical water at 580 - 600 °C and 25 MPa for 50 and 1000 h. The conductivity of SCW was analyzed to be lower than 0.1 μS/cm and the pH was ~ 9.2 adjusted by borate buffer. The samples exposed for 1000 h were subsequently cross-sectioned and metallographicaly prepared for observation by using light and electron microscopy (SEM; TESCAN VEGA TS 5130 XM). The oxide layers were further analyzed by X-ray photoelectron spectroscopy (XPS; ESCA Probe P Instrument) with Al anode and monochromator. The chemical composition of formed oxide layer was also studied by the Raman spectroscopy (Labram HR). The properties of the oxide layers formed on the samples during exposition under SCW were studied by electrochemical impedance spectroscopy (EIS).

All EIS and other electrochemical measurements were performed in three-electrode arrangement. The working electrode (WE) was the studied material - HR3C. The counter electrode (CE) was Pt wire wound coaxially around the WE. The Ag/AgCl electrode, filled with saturated KCl was used as the reference electrode (RE). EIS measurements were carried out at open circuit potential (OCP) in the frequency range from 100 000 to 0.001 Hz at an amplitude of 5 mV.

Furthermore, electrochemical potential-kinetic repassivation method was used to verify the sensitivity to intergranular corrosion in the solution of sulphuric acid and potassium cyanate. The level of sensitization was determined from the ratio of the critical current density reactivating (current maximum of the reverse polarization curve) and the passivation density (current maximum of the anodic polarization curve).

3. RESULTS AND DISCUSSION

Fig. 1 shows the initial microstructure of welded HR3C. The microstructure of HR3C consists of austenitic grains and some phases like nitrides and carbides of Nb and Cr are also present. The weld exhibits dendritic structure without defects. As the heat affected zone (HAZ) could not be clearly defined on the basis of LM analyses, the microhardness profile was used for this purpose.

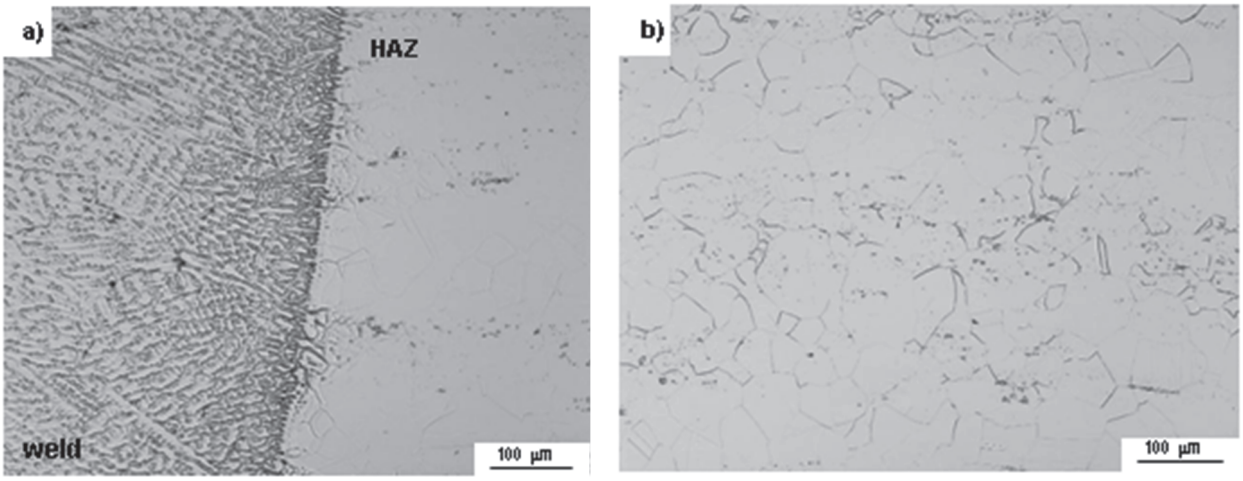

Fig. 1 Microstructure of as-received welded HR3C: (a) weld, (b) base material

Fig. 2 shows the microstructure of the welded sample and base material HR3C after the exposition under SCW for 1000 h. The supercritical water environment led to precipitation of the fine carbides predominately at the grains boundaries. These fine carbides - probably $Cr_{23}C_6$ [5, 9] - formed network and they were rarely found within the grains. Microstructure of the weld seems to be unaffected.

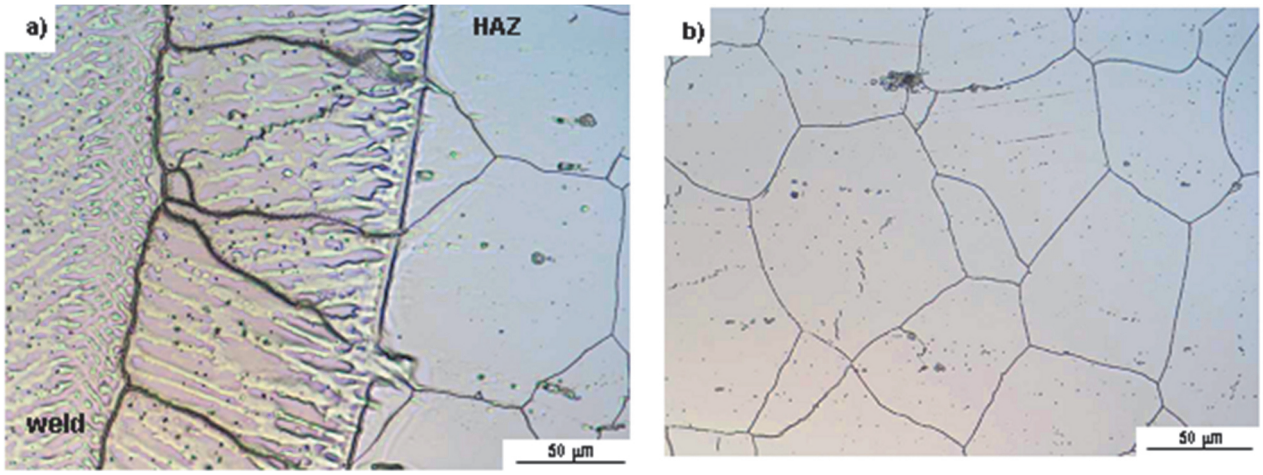

Fig. 2 Microstructure of welded HR3C after exposition under SCW for 1000 h: (a) weld, (b) base material

The measured microhardness MHV 0,1 was 230 ± 6 for the base HR3C material and 265 ± 13 for the weld, respectively. The values of microhardness are only slightly influenced by the exposition experiments as the changes remain within the estimated standard deviation (e.g. 223 ± 7 for base HR3C material and 273 ± 16 for weld).

Insignificant weight changes were observed after the exposition in SCW for 1000h. The total weight gain was approximately 0,00147g. The corrosion rate was estimated to be 0.0007 mm per year. However, the oxide layer formed during the exposition was very thin and difficult to observe or analyse by SEM.

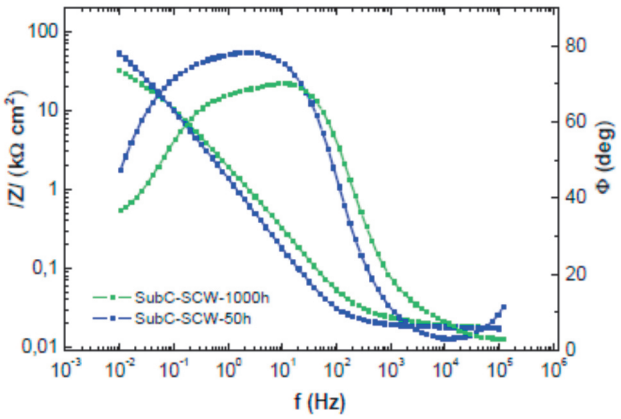

Fig. 3 Impedance spectra of welded HR3C after exposition in supercritical water for 50 and 1000 hours as Bode diagram

Therefore, to broaden the data related to corrosion behaviour of the HR3C, the electrochemical impedance spectra for welded HR3C exposed for 50 and 1000 h were measured and they are shown in **Fig. 3**. On the basis of Bode plot, the oxides generated under SCW conditions show a higher degree of dispersion influenced probably by the transition from sub up to supercritical conditions. The impedance spectra of exposed samples show the separating of spectra into two time constants, even after 50 hours of exposition. The reason is probably duplex nature of the formed oxides. In addition, the longer exposition leads to increasing of the mentioned separation. Thus it can be suggested, that thinner and more compact layer is formed at the beginning of the exposition. This layer has predominantly topotactic character. It is followed by formation of epitactic oxide layer with different charge transfer properties.

The given shape of impedance dispersion (**Fig. 3**) can be characterized by equivalent circuits schematically shown in **Fig. 4**.

where Rs is the solution resistance, R_1 is resistance of the formed layer. In the simple case (**Fig. 4a**), R_1 is equal to polarization resistance R_P. In the second case (**Fig. 4b**) corresponding to spectrum measured after long exposition (1000 h), the R_p is equal to the arithmetic sum of R_1 an R_2. The level of impedance dispersion is possible to quantify based on application of the so-calledconstant-phase element (CPE). CPE can be quantified via following equation (1):

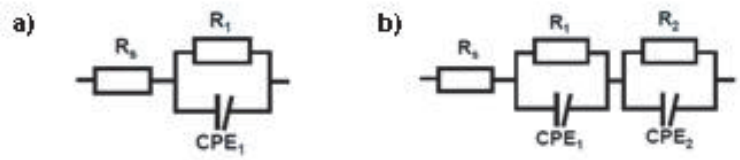

Fig. 4 Used equivalent circuits for fitting EIS date in the case of 50h (a) and 1000 h (h) exposition

$$Z_{CPE} = 1/\sigma\,(j\omega)^{-n} \qquad 1)$$

where σ is the CPE coefficient, n is the exponent of CPE, j is the imaginary unit and ω is the angular frequency. The CPE exponent n having value from 0 up to 1 (n=1 corresponding to an ideal capacitance, e.g. in the case of smooth surface). CPE is connected in parallel to *Rx* and represents a part of non-faradaic electrode phenomena—namely the response of a non-ideal (dispersive) double layer capacitance.

It was found that values of *Rp* of formed oxide layer decrease with increasing exposition time as well as exponent CPE. Such changes indicate that the formation of oxides can be influenced by the changes occurring in the microstructure during exposition under SCW. As was mentioned above, during long-term exposition the chromium carbides are formed. Thus, the distribution of chromium is not uniform, which may affect the process and properties of formed oxide layer. It can be connected with the sensitization, which was confirmed by the electrochemical repassivation tests. The results of these tests reveal that the level of sensitization is about 30 % after exposition under SCW for 1000 h. This was further confirmed by LM identifying attached grain

boundaries. In addition, the equivalent circuit (**Fig. 4b**) in the case of longer exposition indicates the existence of two interfaces, which can be connected with that the oxide shows

transfer characteristics of a duplex layer. In addition, defects can be formed during long exposition, which influences charge transfer properties of the oxide layer and thus the values of *Rp* and *n* are decreased as was mentioned above.

The chemical composition of the formed oxide layer was further studied by the Raman spectroscopy and XPS. Based on Raman spectroscopy it was found that oxide layer formed during exposition for 50 h is composed predominantly by $FeCr_2O_3$. With increasing exposition time, the composition is slightly modified and Cr_2O_3 is also present. In **Fig. 5** concentration profile of oxide layer formed on the welded HR3C steel exposed under SCW for 50 h is shown. It can be seen that small amount of Ni is also present in the formed oxide layer.

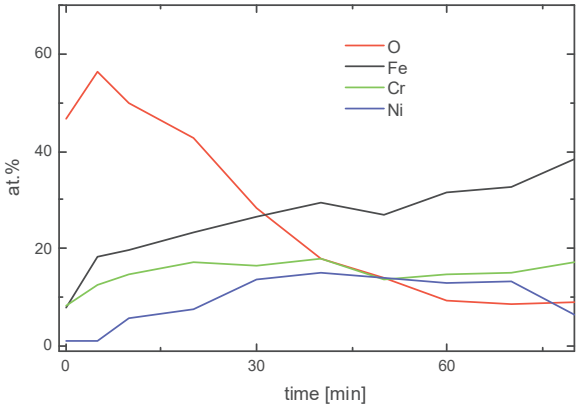

Fig. 5 Concentration profile of oxide layer formed on the HR3C steel exposed under SCW for 50 h (XPS analysis)

CONCLUSIONS

Welded samples of HR3C with mechanically treated surfaces were exposed in SCW at 580 - 600 °C and 25 MPa up to 1000 h. The corrosion behaviour was studied based on weight, microstructure and microhardness changes and analyses such as EIS, XPS and Raman spectroscopy.

It was found that weld is not significantly influenced by long term exposition. In contrast, fine carbides of chromium are formed predominantly at grain boundaries and rarely within grain of austenitic base material. The oxide layer formed during long term (1000 h) is very thin and estimated corrosion rate is acceptable.

The composition and properties of oxide layer formed under SCW conditions is influenced by the time of exposition. Thus, the oxide layer formed during 50 h exposition is predominantly composed by FeCr2O3 and seems to be more compact according to EIS. In contrast, long term exposition leads to formation of duplex layer containing defects and consisting of Cr2O3 next to FeCr2O3.

In spite of that, it can be concluded that HR3C exhibits very good corrosion behaviour under SCW condition. Therefore additional tests such as stress corrosion cracking and slow strain rate tests are planned under such conditions.

ACKNOWLEDGEMENTS

This work has been supported by the SUSEN Project CZ.1.05/2.1.00/03.0108 (ERDF) and PRAMEK Project TA02021406.

REFERENCES

[1] Kritzer, P. Corrosion in high-temperature and supercritical water and aqueous solutions: a review, Journal of Supercritical Fluids, 29, 1-2, 2004, 1-29.

[2] YAN, B., WU, J., XIE, Ch., HE, F., WEI. Ch. Supercritical water gasification with Ni/ZrO2 catalyst for hydrogen production from wastewater of polyethylene glycol. Journal of Supercritical Fluids, 50, 2, 2009, 155-161.

[3] SUN, Ch., R. HUI, W. QU, S. YICK. Progress in corrosion resistant materials for supercritical water reactors. Corrosion Science, 51, 11, 2009, 2508-2523.

[4] Ehrlich, K., Konys, J., Heikinheimo, L. Materials for high performance light water reactos, J. Nucl. Mater., 327, 2-3, 2004, 140-147.

[5] Chi, Ch., Yu, H., Xie, X. (2011). Advanced Austenitic Heat-Resistant Steels for Ultra-Super-Critical (USC) Fossil Power Plants, Alloy Steel - Properties and Use, Dr. Eduardo Valencia Morales (Ed.), InTech, DOI: 10.5772/28412. Available: http://www.intechopen.com/books/alloy-steel-properties-and-use/advanced-austenitic-heat-resistant-steels-for-ultra-super-critical-usc-fossil-power-plants.

[6] VISWANATHAN, R., BAKKER, W. Materials for Ultrasupercritical Coal Power Plants - Boiler Materials: Part 1, 10, 1, 2000, 81-95.

[7] Cao, J., Gong, Y., Yang, Z., Luo, X., Gu, F., Hu, Z. Creep fracture behavior of dissimilar weld joints between T92 martensitic and HR3C austenitic steels. Inter. J.Press. Vess.Pip., 88, 2-3, 2011, 94-98.

[8] Cao, J., Gong, Y., Yang, Z. Microstructural analysis on creep properties of dissimilar materials joints between T92 martensitic and HR3C austenitic steels. Mater.Sci. Eng.A528, 19-20, 2011, 6103-6111.

[9] FANG, Y., ZHAO, J., LI, X. Precipitation in HR3C steel aged at high temperature. Acta Meta.Sinica, 46, 7, 2010, 844-849.

[10] Zieliński, A. Austenitic steels for boiler elements in USC power plants. J.Achiev. Mater. Manufac. Eng., 57, 2, 2013, 68-75.